Supplemental materials:

The role of filopodia in the recognition of nanotopographies

Authors and affiliations:

Jörg Albuschies and Viola Vogel*

Department of Health Sciences and Technology
ETH Zurich
CH-8093 Zurich, Switzerland

*Corresponding author:

Prof. Dr. Viola Vogel
Laboratory of Applied Mechanobiology
Department of Health Sciences and Technology
ETH Zurich
Wolfgang Pauli Strasse 10, HCI F443
CH-8093 Zurich, Switzerland
Phone: +41 44 632 08 87
Fax: +41 44 632 10 73
E-Mail: viola.vogel@hest.ethz.ch

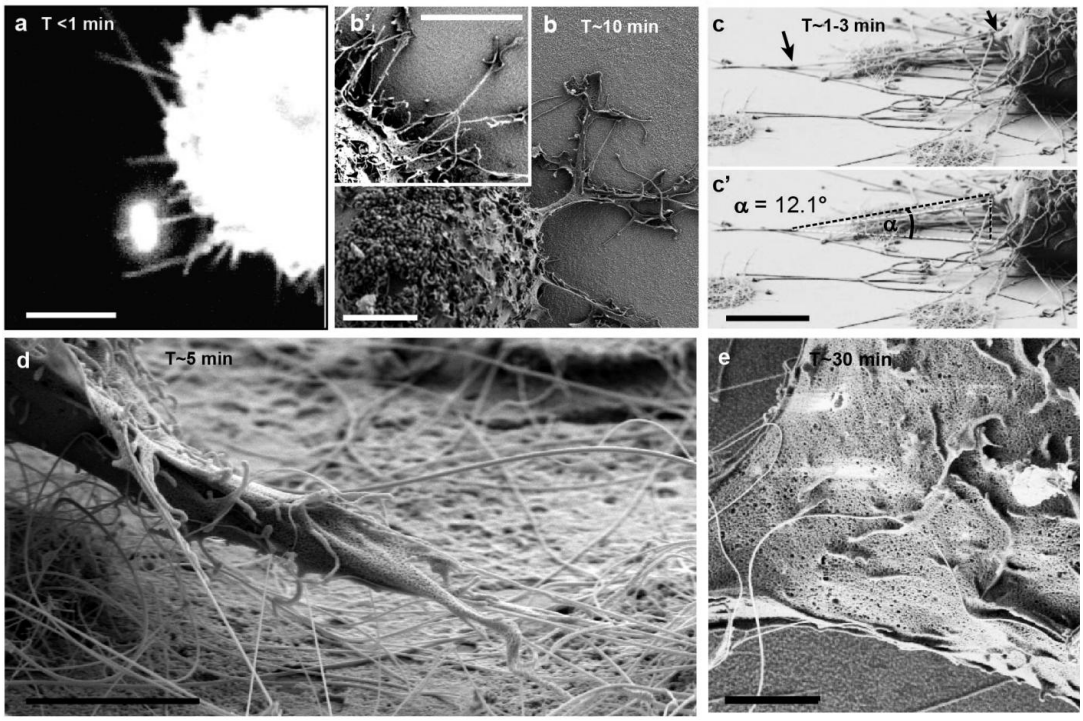

Suppl. Fig. S1: Randomly protruding filopodia control different cell responses during spreading on or within different matrix topographies

(a) 2D projection of a 3D confocal z-stack reconstruction of randomly prodruding filopodia from the surface of a spherical fibroblast before spreading. (b) Lamellipodia-like protrusions outgrowing along filopodia. (c) Filopodia contact angles on flat surfaces: only few filopodia protruding from the surface of spherical cells formed stable adheions while most filopodia peeled off. (d) Membrane protrusion/pseudopod guidance via aligned filopodia-nanowire contacts. Individual nanowires aligned with single filopodia as cells applied traction forces. Firm substrate contacts initiated membrane protrusions towards the site of anchorage. (e) Ruffle formation after filopodia retraction: Membran ruffles occured after approx. 30min along membrane regions where tranasient filopodia had retracted. These membrane ruffles lead to lamellipodia formation which initiated cell migration towards neighboring flat surface areas. Scale bars a, b, c = 5 μm; d = 3 μm; e = 2 μm

Derivation of the contact angle model how filopodia sense topogragphies

Variables

Filopodium-substrate contact angle: α

Filopodia traction force: $\boldsymbol{F}_f = F_l + F_n$

Lateral force component: $F_l = \boldsymbol{F}_f \cos\alpha$

Normal force component: $F_n = \boldsymbol{F}_f \sin\alpha$

Projected cross-sectional area: $A_p = {D_f}^2 \cot\alpha$

Number of integrins within A_p: $N_{ni} = (D_f + x_t) \cdot (D_f \cot\alpha + x_l) \cdot \frac{1}{x_t \cdot x_l}$

Normal force on one integrin: $F_{ni} = \frac{F_n}{N_{ni}} = \frac{\boldsymbol{F}_f \sin\alpha}{(D_f + x_t) \cdot (D_f \cot\alpha + x_l) \cdot \frac{1}{x_t \cdot x_l}}$

Lateral force on one integrin: $F_{li} = \frac{\boldsymbol{F}_l}{total\ number\ of\ engaged\ integrins}$

A filopodium that contacts an object, including flat surfaces or nanofibers, applies a traction force to this anchorage via a cross-linked actin cable inside the filopodium. Randomly protruding filopodia of spherical cells can contact surfaces under an angle α and pull on the contact with the traction force vector $\boldsymbol{F}_f$ that is directed towards the cell body. $\boldsymbol{F}_f$ acting on the adherent filopodium thus has a lateral and a normal component, F_l and F_n relative to the object surface. For simplicity we assumed that the force is equally distributed over all cross-linked actin filaments within the cross-section of a filopodium and that normally acting force component will be equally distributed over all ligand-receptor interactions within the projected area A_p as illustrated in Fig. 5e. The lateral force component is equally distributed over all engaged integrins along the filopodium length in contact with the surface also outside of the projected area A_p.

Estimated numbers derived from our data and the literature

Filopodia traction force:	F_f	= 2 nN
Diameter of fibroblast filopodia:	D_f	= 110 nm
Transversal integrin spacing:	X_t	= 36 nm
Lateral integrin spacing:	X_l	= 36/60 nm

Background information from which the estimated values were derived

Force distribution at site of filopodium adhesion: The integrins within the adhesive and surface-aligned part of the filopodium are coupled to a cross-linked actin cable rather than to individual actin filaments. If the elastic modulus of actin would be infinite, then the lateral force component F_l (shear) is equally distributed over all surface adherent integrins at the filopodia-substrate contact. The elastic modulus E of actin filaments is indeed rather high. The stiffness of a 1 μm long filament was determined in vitro to be 43.7 ± 4.6 pN/nm. (Kojima et al., 1994)[1]. As the total number of engaged integrins increases, the lateral force component per individual integrin will be progressively small.

F_n: The normal force component F_n acts only on those integrins which are located within the projected area of the filopodium cross-section as depicted in figure 5e.

Considerations about integrin orientation and shear vs. normal forces

Since it is not known whether individual integrin-FN bonds are more susceptible to breaking under either normal or shear forces, we tried to estimate the total forces acting on individual integrins. The geometry by which the forces are pulling on the proximal ends of filopodia that are either aligned with the object or are touching it under a tilt angle, affects how the force is distributed over the many bonds that are formed and whether they can be broken. By the vectorial separation of forces into lateral and normal components it is shown that the strongest forces on individual integrins are the normal forces at elevated angles. The normal force component is just applied to a limited number of integrins in the kink region, whereas the lateral component is equally distributed over all surface attached integrins and has thus a much smaller contribution to the total force that is acting on individual integrins.

Once the normal versus lateral rupture force components have been measured experimentally, our model can easily be adapted to include an angle-dependent correction factor.

Estimation of integrin density at filopodia surface adhesions

Longitudinal integrin spacing x_l: Since the integrin density in filopodial adhesions are unknown, we calculated two cases. First, we assumed that the maximum integrin density along an actin filament is given by the periodicity of the actin super helix repeat with a length of 36-37.5 nm (Volkmann et al., 2001)[2]. A value around 35-37 nm also corresponds well to integrin densities within focal adhesions (Patla et al., 2010)[5]. Second, we assumed an upper integrin spacing of 60 nm that is required for FAs to form and mature (Arnold et al., 2008, 2004)[3,4].

Transversal integrin spacing x_t: Actin filaments within filopodia are separated by actin cross-linking proteins, e. g. 12-13 nm by fascin (Cant et al., 1994; DeRosier and Edds, 1980)[6,7]. Here, we assumed an equally spaced integrin density (transversal and longitudinal) with a spacing of 36 nm (3x12 nm spacing).

Number of integrins per row: Taking a filopodium diameter D_f of 110 nm (measured with SEM), we get a maximum of four parallel integrins (x_t = 36 nm) across the diameter, which are contributing to the filopodium adhesion on a flat surface 110 $nm \sim= 3 \cdot 36\ nm + 5\ nm$ (lipid membrane).

Kink angle dependencies: If we assume that the tractional force $\boldsymbol{F_f}$ of the filopodium is constant, the force F_n and F_l are functions of the tilt angle α. The projected force area A_p and therefore the number of integrins experiencing F_n is also a function of α. N_{ni} is the total number of integrins which are located within A_p and therefore experiencing F_n. The diameter of the filopodium is assumed constant (as measured): D_f = 110 nm.

The total number of integrins is unknown, but for longer sections of adhering filopodia shafts, which could be observed experimentally (several micrometer), the number increases and is much larger than N_{ni}. Therefore the lateral force component F_{li} will become very small and can be neglected for the determination of forces in the projected cross-section area. The total force on one integrin in the projected adhesive cross-section area is therefore approximately F_{ni}:

$$F_{ni}(\alpha) = \frac{\boldsymbol{F}_f \sin\alpha}{\left(D_f + \mathrm{x}_t\right) \cdot \left(D_f \cot\alpha + x_l\right) \cdot \frac{1}{x_t \cdot x_l}}$$

This formula allows us now to calculate the force per integrin in dependency of the contact angle α.

The force acting on one integrin in the kink area is plotted as a function of α (Figure 5f) by assuming a filopodia traction force of 2 nN and two different integrin densities. To estimate the critical contact angle below which peeling will stall, we next assumed that the integrins within the filopodial shaft can sustain the same force as in focal adhesions (FAs). Cells typically apply traction forces of about 5 nN/μm^2 at focal adhesions (FA) (as reviewed in Bershadsky et al., 2003)[10]. This converts to a force per integrin of about 6/10 pN (as marked in Figure 5f with red squares for the two assumed integrin densities,

i.e. 507 or 827 integrins per μm^2). This set of assumptions predicts a critical angle of 12° below which filopodium-substrate interactions might be able to sustain the tensile forces without beeing ruptured open. On flat surfaces or at filopodia-nanowire contacts, we typically observed that the forces were building within a few minutes. Assuming that the force has reached a plateau at 1.9 nN, we obtain a loading rate of roughly 6-10 pN/s.

Measurement of filopodia contact angles

The contact angle of filopodia touching a flat surface can be estimated from SEM images, but it is difficult to quantify them because we do not know the history of the contact, i.e. whether is was in a peeling or stabilized mode at the time of cell fixation. Additionally, a rotational error might be introduced since the SEM side view alone does not deliver a direct perpendicular view onto the plane defined by the filopodial angle. In the SEM image shown in Suppl. Fig 1c, the peeling process might have been terminated as indicated by the advancing membrane protrusion seen at the root of the filopodium. The measured angle was corrected for the sample tilt of 23° during SEM imaging (black dashed line). The contact angle for this example still shows an error of approx. 10% due to the unspecified rotational position of the filopodium around the surface normal axis.

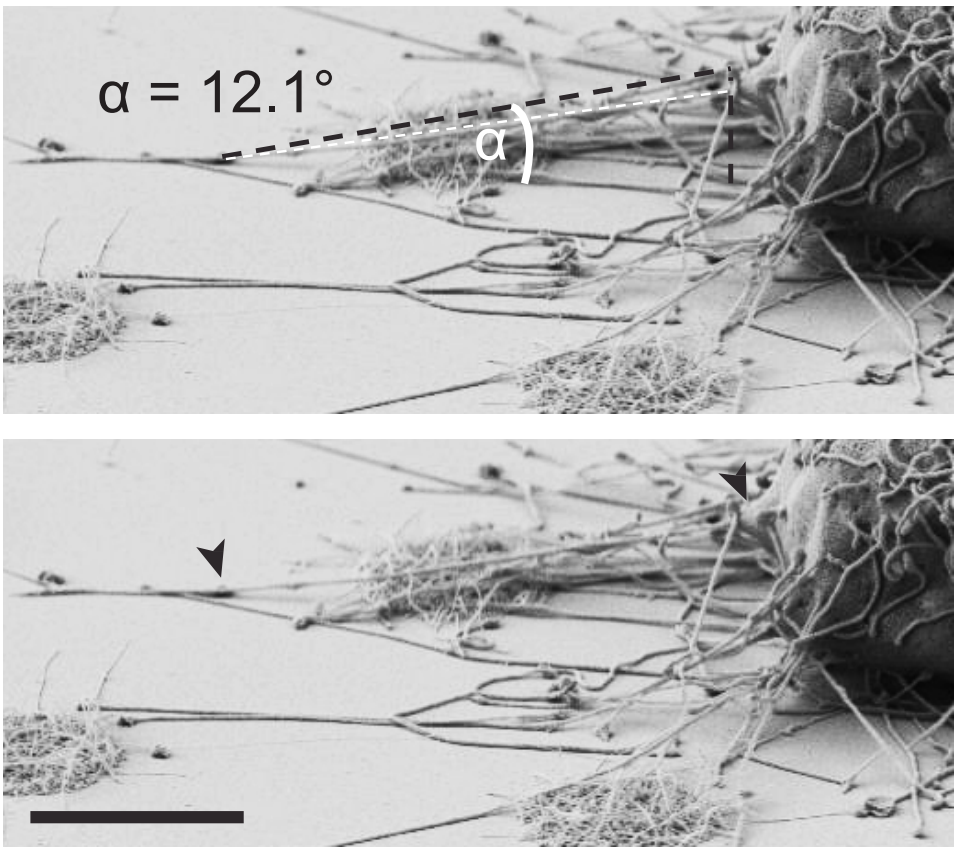

Suppl. Fig. 1c: Contact angle determination from side view SEM micrographs. The suspended length of the filopodium between the cell cortex and the substrate contact (arrowheads) is 13 μm. Scale bar 5 μm

References

1 Kojima, H., Ishijima, A. & Yanagida, T. Direct measurement of stiffness of single actin filaments with and without tropomyosin by in vitro nanomanipulation. *Proc Natl Acad Sci U S A* **91**, 12962-12966 (1994).

2 Volkmann, N., DeRosier, D., Matsudaira, P. & Hanein, D. An atomic model of actin filaments cross-linked by fimbrin and its implications for bundle assembly and function. *J Cell Biol* **153**, 947-956 (2001).

3 Arnold, M. *et al.* Induction of cell polarization and migration by a gradient of nanoscale variations in adhesive ligand spacing. *nano letters* **8**, 2063-2069 (2008).

4 Arnold, M. *et al.* Activation of integrin function by nanopatterned adhesive interfaces. *Chemphyschem : a European journal of chemical physics and physical*

chemistry **5**, 383-388, doi:10.1002/cphc.200301014 (2004).
5 Patla, I. *et al.* Dissecting the molecular architecture of integrin adhesion sites by cryo-electron tomography. *Nat Cell Biol* **12**, 909-915, doi:10.1038/ncb2095 (2010).
6 Cant, K., Knowles, B. A., Mooseker, M. S. & Cooley, L. Drosophila Singed, a Fascin Homolog, Is Required for Actin Bundle Formation during Oogenesis and Bristle Extension. *Journal of Cell Biology* **125**, 369-380 (1994).
7 DeRosier, D. J. & Edds, K. T. Evidence for fascin cross-links between the actin filaments in coelomocyte filopodia. *Exp. Cell Res.* **126**, 490-494 (1980).
8 Nordin, D., Donlon, L. & Frankel, D. Characterising single fibronectin-integrin complexes. *Soft Matter* **8**, 6151-6160, doi:Doi 10.1039/C2sm07171a (2012).
9 Li, F., Redick, S. D., Erickson, H. P. & Moy, V. T. Force measurements of the alpha5beta1 integrin-fibronectin interaction. *Biophys J* **84**, 1252-1262, doi:10.1016/S0006-3495(03)74940-6 (2003).
10 Bershadsky, A., Balaban, N. & Geiger, B. Adhesion-dependent cell mechanosensitivity. *Annu. Rev. Cell. Dev. Biol.* **19**, 677-695, doi:10.1146/cellbio.2003.19.issue-1 (2003).
11 Hur, S. S., Zhao, Y., Li, Y. S., Botvinick, E. & Chien, S. Live Cells Exert 3-Dimensional Traction Forces on Their Substrata. *Cell Mol Bioeng* **2**, 425-436 (2009).